Technology and Science for the Ships of the Future
V. Crupi and V. Bucci (Eds.)

doi:10.3233/PMST250038

A B-Spline Rankine Panel Method for the Double-Body Flow Problem Solution for Time Domain Seakeeping Applications

Francesco SOARDI [a,1] and Giuliano VERNENGO [a]
[a] *DITEN, Department of Marine Engineering and Naval Architecture, Polytechnic School of the University of Genoa, Italy*
ORCiD ID: Francesco Soardi https://orcid.org/0009-0003-4201-8815, Giuliano Vernengo https://orcid.org/0000-0001-8191-8742

Abstract. A computationally efficient three-dimensional B-Spline Rankine Panel Method (B-RPM), tailored for solving the double-body flow problem in marine hydrodynamics and seakeeping scenarios with a free surface, is presented. The double-body flow, which is the main and time-independent contribution, serves as the basis flow for the overall hydrodynamic problem for time domain ship motions, ruled by the Laplace equation. Initially, a technique was developed that employed constant source distributions to solve the double-body flow. In a subsequent phase, the method is enhanced for problems involving hydrodynamic circulation by incorporating B-Spline sources and normal dipoles distributions on both body and free surfaces. An integral approach has been devised, leveraging the second Green identity and constant sources distribution to address double-body flow and evaluate potential second derivatives on the free surface, respectively. While focused on simple geometries for initial simulations and validation, this work marks the first stage of a broader time-domain model. The findings demonstrate that the B-RPM enables achieving comparable results with fewer panels than traditional constant source distribution methods. Additionally, it makes the direct analytical calculation of potential derivatives possible.

Keywords. B-Spline, Rankine Panel Method, Time domain simulations, Ship motions, Computational hydrodynamics, Double-Body flow, Potential flow theory

1. Introduction

Since the pioneering work of [1], panel methods have been widely used to solve hydrodynamic problems and analyze 3D flows around bodies of arbitrary shape. A classical approach employs the free surface Green function, with significant contributions from [2], [3] and [4]. An efficient alternative is represented by the Rankine Panel Method (RPM), which uses Rankine sources distributed over the boundary surfaces. This choice simplifies kernels evaluation and offers more flexibility in enforcing free surface conditions.

[1] Corresponding Author: Francesco Soardi, francesco.soardi@edu.unige.it.

The use of RPM in seakeeping originated with [5], who introduced a B-Spline-based discretization. Unlike the Constant RPM (C-RPM), the B-Spline RPM (B-RPM) expresses unknowns using quadratic basis functions modulated by spline coefficients, ensuring continuity and enabling analytical evaluation of first and second derivatives. Finally, the Weak-Scatterer model, introduced by [6], represents a natural evolution of the above model.

In the present work, a B-RPM is developed and tested within the full linear time-domain framework, focusing on steady wave flow solution based on the double-body flow linearization proposed originally by [7] and [8]. Different numerical solutions are compared, and an innovative method is proposed to compute second vertical derivatives of the double-body flow potential on the free surface, avoiding finite difference approximations. This study contributes to a broader effort toward a partially nonlinear time-domain model that combines full linear and weak-scatterer approaches for large-amplitude motions analysis.

2. Mathematical Formulation

A right-handed orthonormal reference system, $O-xyz$, is introduced, which is steadily translating with respect to an external reference system fixed in space, at the mean speed of the body, $\vec{U}$. In this work, all equations will be referred to this inertial steady translating reference system. The origin, O, is placed on the undisturbed free surface plane, $\mathscr{F}_0$, or $z=0$. According to exact formulation of the hydrodynamic problem based on the potential flow theory, the total velocity potential, $\Psi(\vec{x};t)$, must satisfy the Laplacian in all the fluid domain, $\mathscr{D}$, and a series of non-linear boundary conditions over the instantaneous free surface elevation, $\mathscr{F}$, or $z=\zeta(x,y;t)$ and, on the exact body surface, $\mathscr{H}$. These boundary conditions result in the following:

$$\left[\frac{\partial}{\partial t}-(\vec{U}-\nabla\Psi)\cdot\nabla\right]\begin{Bmatrix} z-\eta(x,y;t) \\ \Psi(\vec{x};t)\end{Bmatrix}=\begin{Bmatrix} 0 \\ \frac{1}{2}|\nabla\Psi|^2-g\zeta\end{Bmatrix} \quad \text{on} \quad z=\eta(x,y;t), \tag{1}$$

$$\vec{n}\cdot\nabla\Psi=\vec{n}\cdot\frac{\partial\vec{\delta}}{\partial t}+\vec{n}\cdot\vec{U} \quad \text{on} \quad \mathscr{H}, \tag{2}$$

where η is the instantaneous wave elevation and $\delta(\vec{x};t)$ is the rigid displacement of a generic point of $\mathscr{H}$. To make the present formulation complete, a bottom condition, if considered, and a decay radiation condition at infinity, are necessary.

2.1. The Linear Time Domain Model Formulation

Involving linearity of the Laplace operator, a general accepted decomposition for total velocity potential and wave elevation can be formulated as follow:

$$\Psi(\vec{x};t)=\Phi(\vec{x};t)+\phi(\vec{x};t)+\psi(\vec{x};t)+\psi^e(\vec{x};t), \tag{3}$$

$$\eta(\vec{x};t)=\zeta(\vec{x};t)+\zeta^e(\vec{x};t), \tag{4}$$

where Φ is the double-body or basis flow potential, ϕ the local flow potential (representative of the impulsive response of the body to motions and velocities), ψ and ζ are

the memory or wave flow quantities, and ψ^e and ζ^e are the incident wave quantities. Decompositions in Eqs. (3) and (4), which can also be found in [9], [10] and [11], are valid for both linear and weak-scatterer models. However, the main difference between the two models lies in the size of the single terms. In the linear time domain model, the main contribution to the total flow is assumed to be the double-body flow, $\Phi \sim \mathscr{O}(1)$, and all other remaining terms in Eq. (4) are considered as small perturbations, that is: $\phi, \psi, \psi^e \sim \mathscr{O}(\varepsilon)$ and $\zeta, \zeta^e \sim \mathscr{O}(\varepsilon)$ with $\varepsilon \ll 1$. In addition, during a forced periodic motion simulation, the time story for each rigid-body mode is prescribed, so only the wave field is solved, and its solution is independent of the integration of equations of motion. In this case, the incident, diffraction, and radiation contributions are implicitly derived by solution of the local and memory flows, whereby the linearised boundary conditions are obtained by neglecting incident terms in Eqs. (3) and (4).

With these considerations, boundary conditions for the linear model are derived by substituting Eqs. (3) and (4) within the conditions in Eqs. (1) and, after neglecting the terms of order ε^2, transferring them to the plane $z = 0$ by applying a Taylor expansion for small η. The result of the above process, neglected incident terms, produces the following evolution equations:

$$\left[\frac{\partial}{\partial t} - (\vec{U} - \nabla\Phi)\cdot\nabla\right]\zeta = \frac{\partial^2\Phi}{\partial z^2}\zeta + \frac{\partial\phi}{\partial z} + \frac{\partial\psi}{\partial z} \quad \text{on} \quad z = 0, \tag{5}$$

$$\left[\frac{\partial}{\partial t} - (\vec{U} - \nabla\Phi)\cdot\nabla\right]\psi = \vec{U}\cdot\nabla\Phi - \frac{1}{2}\nabla\Phi\cdot\nabla\Phi - g\zeta \quad \text{on} \quad z = 0. \tag{6}$$

In the derivation of the above expressions three conditions were adopted: the double-body flow rigid-wall condition, $\Phi_z = 0$ on $z = 0$, the time indipendence of the basis-flow (in contrast with weak-scatterer model), $\Phi_t = 0$, and the null local pressure condition, $\phi = 0$ on $z = 0$, which implies the cancellation of the convective term involving ϕ in the second condition in Eq. (1). In a steady forward motion simulation without imposed rigid-body mode, the local flow forcing term in Eq. (5), ϕ_z, can be eliminated. Instead, when the local contribution is present, the decomposition for ϕ proposed by [12] may be adopted.

The body boundary condition in Eq. (2), neglected local and incident terms, is linearised by transferring it from the instantaneous wetted surface, $\mathscr{H}$, to the mean body position, $\mathscr{H}_0$, where the following balances are imposed:

$$\vec{n}\cdot\nabla\Phi = \vec{n}\cdot\vec{U} \quad \text{on} \quad \mathscr{H}_0, \tag{7}$$

$$\vec{n}\cdot\nabla\psi = 0 \quad \text{on} \quad \mathscr{H}_0, \tag{8}$$

here $\vec{n}$ denotes the outward normal to body surface $\mathscr{H}_0$.

2.2. *The Boundary Integral Formulation*

In Eqs. (5) and (6), ψ, ψ_z, and ζ, which fully characterize the wave field, are unknowns of the problem. The third equation that completes the mathematical formulation can be derived from the second Green's identity, which provides the following boundary integral formulation in terms of the total velocity potential (see e.g. [13]):

$$2\pi\Psi(\vec{x};t) - \iint_{\mathscr{F}_0\cup\mathscr{H}_0} [\vec{n}\cdot\nabla_\sigma\Psi(\vec{\sigma};t)]\,G(\vec{x};\vec{\sigma})\,d\sigma + \iint_{\mathscr{F}_0\cup\mathscr{H}_0} \Psi(\vec{\sigma};t)\,[\vec{n}\cdot\nabla_\sigma G(\vec{x};\vec{\sigma})]\,d\sigma = 0 \quad \text{for} \quad \vec{x}\in\mathscr{F}_0\cup\mathscr{H}_0, \tag{9}$$

where $G(\vec{x};\vec{\sigma}) = |\vec{x}-\vec{\sigma}|^{-1}$ is the Rankine potential source with $\vec{x}$ and $\vec{\sigma}$ the field and source point, respectively. Formulation in Eq. (9) is suitable for the basis, local, and memory flow problem according to the linear decomposition in Eq. (3). Note that the basis and local flow problems are preparatory to the solution of the memory flow.

3. Numerical Solution of the Wave Field Problem

After obtaining the basis and local flow solution, the system of Eqs. (5), (6), and (9) is solved for each time step for ψ, ψ_z, and ζ on $\mathscr{F}_0$, and for ψ on $\mathscr{H}_0$. The solution scheme consists of discretising the free surface and body surface with a collection of flat quadrangular panels and then collocating, in sequence, Eqs. (5), (6), and (9), in the centroid of each panel on $\mathscr{F}_0$ and $\mathscr{H}_0$. Assuming $t = t_{n+1}$ with $n \geq 0$ the present time, the integration of the evolution equations is carried out via an Emplicit Euler scheme, which first involves the integration of Eq. (5) to update ζ at the time $t = t_{n+1}$ by explicit Euler method using the previous value of ψ_z, and ζ, and then integrating Eq. (6) via implicit Euler scheme to obtain the value of ψ on $\mathscr{F}_0$, at the time $t = t_{n+1}$. Later, ψ on $\mathscr{H}_0$ and ψ_z on $\mathscr{F}_0$, at the time $t = t_{n+1}$, are obtained from the solution of Eq. (9).

The numerical solution for the wave flow problem is achieved using a B-RPM in which all unknowns are distributed over the control surfaces using a B-Spline representation. The generic unknown, $q(\vec{x};t)$, is distributed over each generic-shape quadrangular panel in the local non-orthogonal coordinates, $\{\xi,\eta,0\}$, which discretising the surfaces $\mathscr{F}_0$ and $\mathscr{H}_0$ using quadratic basis functions modulated by appropriate time-dependent spline coefficients as follows:

$$q^{(j)}(\xi,\eta;t) = \sum_{k=1}^{9} q_{j_k}(t) \sum_{m=0}^{2}\sum_{n=0}^{2} \Omega(m,n;k) \left[\frac{\xi}{\delta_\xi^{(j)}}\right]^m \left[\frac{\eta}{\delta_\eta^{(j)}}\right]^n. \tag{10}$$

In equation above, the unknown quantity $q^{(j)}$ is distributed on the $j-$th panel with $j_5 \equiv j$, here $b_{j_k}^{(2)}(\xi)$ and $b_{j_k}^{(2)}(\eta)$ are the local basis functions of second order obtained from a direct manipulation of the global basis functions derived recursively by the convolution integral of Threfeten (1988). The spline coefficients are denoted with $q_{j_k}(t)$, $\delta_\xi^{(j)}$ and $\delta_\eta^{(j)}$ are the mean dimension of the $j-$th panel, and $\Omega(m,n;k)$ are algebraic coefficients obtained from the combination of the local basis functions (see [14] for more details). Due to the superposition of the different basis functions, tangential derivatives of order one and two are obtained by direct derivation of Eq. (10) in the non-orthogonal local reference system, and, after a Jacobian transformation, in the local orthogonal reference of panels, $\{s,t,0\}$, by which the velocity field is evaluated. Numerical solution of the wave flow is obtained by substituting Eq. (10) for the unknowns ψ, ψ_z, and ζ inside Eqs. (5), (6), and (9). More details about this solution scheme can be found in [10], in [11], and in [14]. Employing Eq. (10) makes using the B-RPM for the wave flow problem

preferable, while only the basis and local flow problems are also suitable for the classical source method solution.

3.1. Constant Rankine Panel Method for the Double-Body Flow Solution

The double-body flow problem satisfies, the Laplacian in $\mathscr{D}$, Eq. (7) on $\mathscr{H}_0$ and condition $\Phi_z = 0$ on $\mathscr{F}_0$. Loosing circulation, double-body flow may be solved simply by distributing Rankine sources on $\mathscr{H}_0$ and its image with respect to the plane $z = 0$, $\mathscr{H}_0^*$ (asterisk denotes image quantities). Details about source method are omitted (see Kolz and hess e.g.), anyway, numerical solution is obtained first by applying at each panel centroid of $\mathscr{H}_0$ Eq. (7), and then solving the resulting algebraic system for the unknows sources intensity $Q_j(\vec{\sigma}) = Q_j$ assumed constant on $j-$th panel. In this context, the influence coefficients appear in the following form ($\mathscr{H}_j$ is the $j-$th panel surface):

$$\phi_{mn}^{(j)}(\vec{x}_s(\vec{x})) = \iint_{\mathscr{H}_j} (s-x_s)^m (t-y_s)^n |\vec{x}_s - \vec{\sigma}_s|^{-3} \, ds dt. \tag{11}$$

for $m,n \geq 0$, where $\vec{x}_s = \{x_s, y_s, z_s\}$ and $\vec{\sigma}_s = \{s,t,0\}$ are the field and source point coordinates, respectively, in the local orthogonal reference system of panel. It's straightforward to verify that Φ satisfies the rigid-wall condition on $z = 0$ as, by geometric considerations it appears that: $s_z^{*(j)} = -s_z^{(j)}$, $t_z^{*(j)} = -t_z^{(j)}$ and $n_z^{*(j)} = -n_z^{(j)}$, with $\hat{s} = \{s_x, s_y, s_z\}$, $\hat{t} = \{t_x, t_y, t_z\}$ and $\vec{n} \equiv \hat{n} = \{n_x, n_y, n_z\}$ the $j-$th panel unit versors expressed in the $O-xyz$ base, and, since the problem is symmetric respect the $z = 0$ plane, it reasults also $\phi_{mn}^{*(j)} = \phi_{mn}^{(j)}$, for all $\vec{x} \in \mathscr{F}_0$.

3.2. B-Spline Rankine Panel Method for the Double-Body Flow Solution

For problems involving circulation, the double-body flow solution can be obtained by solving Eq. (9). For this purpose, the B-RPM, used for the wave flow solution, could be a convenient numerical approach. Using Eq. (7), the rigid-wall condition, and Eq. (10), the boundary integral formulation in Eq. (9) is manipulated into the following suitable form for numerical solution for the double-body flow problem (index i identifies the generic quantity evaluated in the $i-$th panel centroid):

$$\begin{aligned} &\sum_{j=1}^{N} \Phi_j \left[\sum_{(h,k)\in\mathscr{V}_j} \left\{ \sum_{m=0}^{2} \sum_{n=0}^{2} \Omega(m,n;k) \frac{D_{ih}^{(m,n)} + D_{ih}^{*(m,n)}}{\delta_\xi^{m(h)} \delta_\eta^{n(h)}} \right\} + 2\pi \sum_{k=1}^{9} \delta_{ji_k} \Omega(0,0;k) \right] \\ &= \sum_{j=1}^{N_H} (\vec{n}^{(j)} \cdot \vec{U}) \left\{ S_{ih}^{(0,0)} + S_{ih}^{*(0,0)} \right\} \end{aligned} \tag{12}$$

for $i = 1, \ldots, N_H + N_F$. Here, Φ_j are the time-independent unknown spline coefficients, $N = N_H + N_F + N_e$, where N_H and N_F are the number of panels distributed over $\mathscr{H}_0$ and $\mathscr{F}_0$, respectively, and N_e denotes the number of the end-spline coefficients. Symbol $\mathscr{V}_j$ indicates a set of nine index pairs, (h,k), containing the number and relative position information of panels adjacent to the $j-$th panel. The unknown spline coefficients are obtained by solution of Eq. (12) after collocating it on the panels centroid arranged on

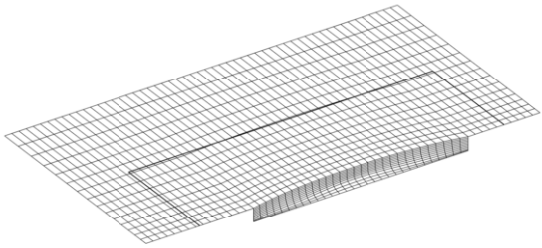

Figure 1. Typical computational mesh.

$\mathscr{F}_0$ and $\mathscr{H}_0$. The quantities, $S_{ih}^{(m,n)}$ and $D_{ih}^{(m,n)}$, are higher-order influence coefficients in the following form ($\mathscr{P}_j$ is the $j-$th panel surface of $\mathscr{F}_0$ or $\mathscr{H}_0$):

$$\begin{Bmatrix} S_j^{(m,n)} \\ D_j^{(m,n)} \end{Bmatrix} (\vec{x}_s\,(\vec{x})) = \begin{Bmatrix} 1 \\ z_s \end{Bmatrix} \iint_{\mathscr{P}_j} (s + t\tan\gamma^{(j)})^m (t\sec\gamma^{(j)})^n \begin{Bmatrix} |\vec{x}_s - \vec{\sigma}_s|^{-1} \\ |\vec{x}_s - \vec{\sigma}_s|^{-3} \end{Bmatrix} ds dt, \quad (13)$$

with $\gamma^{(j)}$ the skew angle of the $j-$th panel. Integrals in Eqs. (11) and (13) have been solved using a procedure described by [15]. To maintain the B-Spline representation at the domain edges consistent, system in Eq. (12) is completed by N_e equations imposed over a single layer of imaginary panels surrounding the truncated domain in all directions. To identify these additional spline coefficients, the natural spline condition of zero end-curvature has been implemented.

3.3. Evaluation of the Vertical Second Derivative of the Double-Body Flow Potential

The B-RPM used in the present work allows the tangential derivatives on the control surfaces to be evaluated accurately, but not the normal ones. The second derivative in Eq. (5) is a fundamental contribution to solving the wave flow problem, and it could be assessed, avoiding the use of the finite difference method, by using the source formulation and introducing an auxiliary potential, such that:

$$\Lambda(\vec{x}) = \Phi_z(\vec{x}) = -\frac{1}{4\pi} \sum_{j=1}^{N_H} Q_{z,j} \left\{ S_j^{(0,0)}(\vec{x}) - S_j^{*(0,0)}(\vec{x}) \right\} \quad \text{for} \quad \vec{x} \in \mathscr{D}. \quad (14)$$

In order to satisfy the rigid-wall condition on $\mathscr{F}_0$, the unknown source intensity are defined so that $Q_{z,j}^* = -Q_{z,j}$, thus for $\vec{x} \in \mathscr{F}_0$, $S_j^{*(0,0)} = S_j^{(0,0)}$ for symmetry, and $\Lambda = \Phi_z = 0$. Using the previous values obtained with the C-RPM or B-RPM procedure for Φ_z evaluated in the centroid of each panel on $\mathscr{H}_0$, the N_H unknown intensities, $Q_{z,j}$, can be obtained from the solution of the system $\Lambda(\vec{x}_i) = \Phi_z(\vec{x}_i)$, for $i = 1, \ldots, N_H$. After that, by direct derivation of Eq. (15), the vertical second derivative of Φ on $\mathscr{F}_0$ is obtained as $\Lambda_z(\vec{x}) = \Phi_{zz}(\vec{x})$. The resulting expression of Φ_{zz} is expressed in terms of the panel moments $\phi_{00}^{*(j)}$, $\phi_{10}^{*(j)}$, and $\phi_{01}^{*(j)}$, defined in Eq. (11).

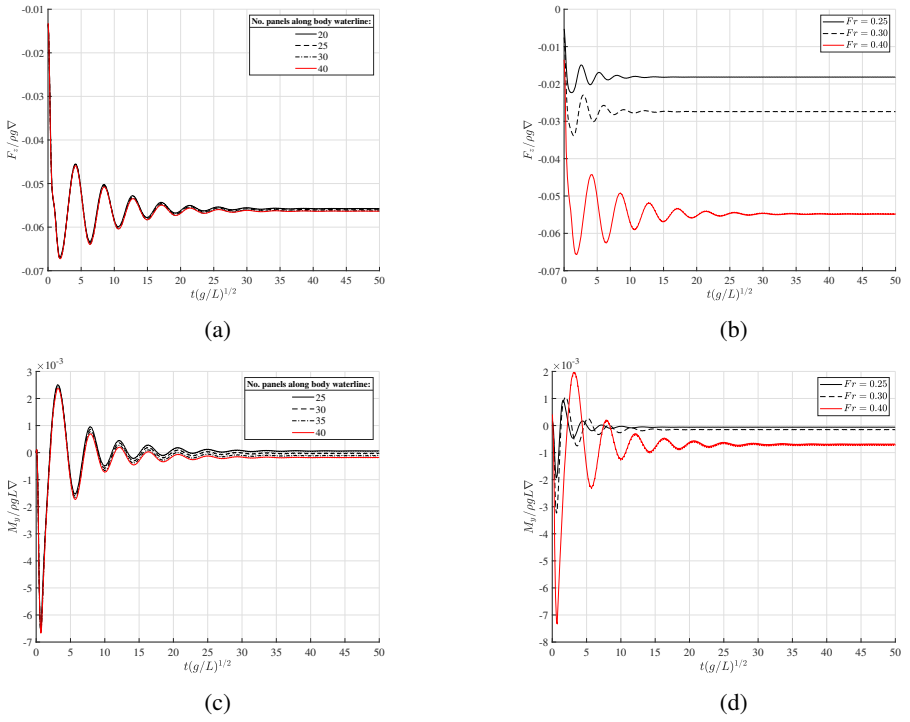

Figure 2. Sensitivity of vertical force (a,b) and pitch moment (c,d) to spatial discretisation and Froude number, Fr.

4. Simulations and Results

A series of forced motion simulations was carried out to validate the consistency of the present B-RPM. The body starts impulsively from rest and reaches the steady speed, U, on a calm free surface. These simulations employed various numerical techniques for numerical force computation, enforcing radiation conditions, and noise filtering for saw-tooth waves. Results include a direct comparison between the C-RPM and B-RPM methods for solving the double-body flow problem; the wave (or memory) flow was addressed using only the present B-RPM. To highlight the differences between the two methods, the analysis focused on steady wave flow based on the linearisation of the double-body flow without external forcing, excluding the local flow solution. Simulations were carried out using Wigley's hull in Journée's Model I configuration to enable rapid validation of the model (e.g., with the results of [10]). A representation of the computational mesh is reported in Figure 1. The numerical beach limit for implementing the radiation condition is also visible. The principle adopted for the realisation of this numerical tool is based on the study of [16], and further details can also be found in [11] and [17].

Hydrodynamic forces were obtained by integrating the linearized pressure over the hull surface, $\mathscr{H}_0$:

$$p_\psi(\vec{x};t) = -\rho\left[\frac{\partial}{\partial t} - (\vec{U} - \nabla\Phi)\cdot\nabla\right]\psi + \rho\left(\vec{U}\cdot\nabla\Phi - \frac{1}{2}\nabla\Phi\cdot\nabla\Phi\right). \tag{15}$$

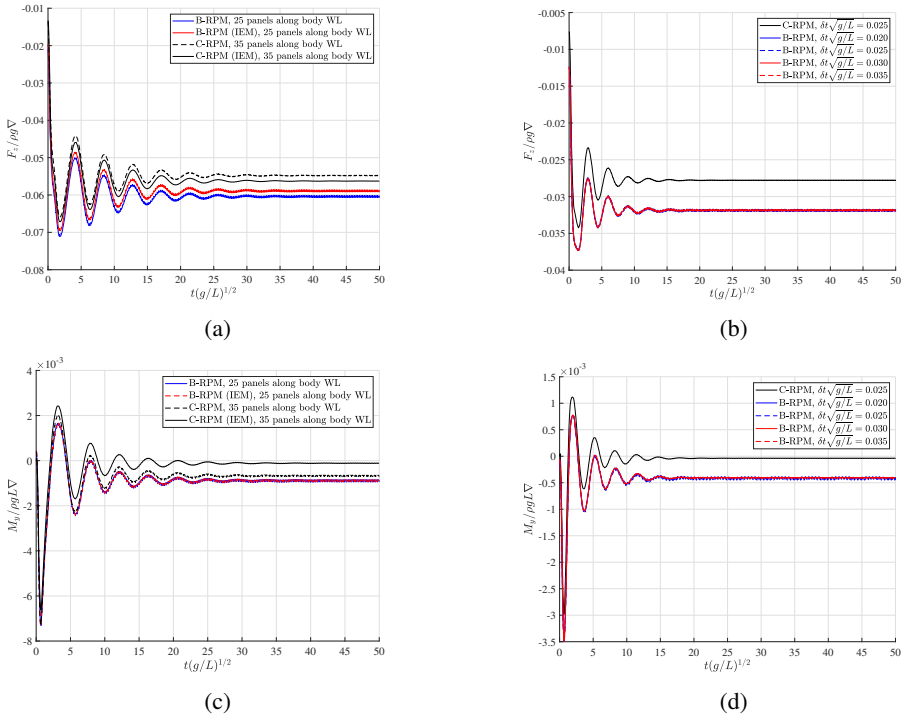

Figure 3. Comparison of C-RPM and B-RPM results in terms of vertical force (a) and pitch moment (c), for $Fr = 0.4$; sensitivity of vertical force (b) and pitch moment (d) to time-step size $\delta t\sqrt{g/L}$, for $Fr = 0.3$.

The wave-induced hydrodynamic force consists of an unsteady memory flow and a predominant steady double-body flow component. The presence of any incident flow should be included in this force, while local contributions are expressed through hydrodynamic coefficients directly within the equations of motion. In free-motion simulations, accurately evaluating the time derivative involving ψ in Eq. (15) is critical (see [18]). Finite-difference schemes can provide sufficiently accurate results, but may lead to instabilities during equations of motion integration, despite the time-step choice. To address this, an integral explicit method (IEM) has been implemented to compute the time derivative in Eq. (15). This approach exploits the harmonicity of the function ψ_t and relies on the application of Eq. (9). Results obtained using this methodology are also presented in this study.

Figure 2 presents the heave force and pitch moment to validate the consistency and sensitivity of the model concerning some simulation parameters. Specifically, Figures 2a and 2c show the influence of the number of panels used for hull discretisation, while Figures 2b and 2d illustrate the effect of the Froude number, $Fr = U/\sqrt{gL}$. For all analyses, the evolution equations were integrated using a time step $\delta t\sqrt{g/L} = 0.025$, which lies well within the stability region for the propagation of the discrete wave field (see, e.g., [15] and [19]). The computed values and trends are consistent with the results reported by [11], and convergence was achieved in all the test cases examined. The size and parameters of the numerical beach were calibrated based on the mean forward speed, U, while the suppression of sawtooth waves was achieved through a 7-point interpolating filter

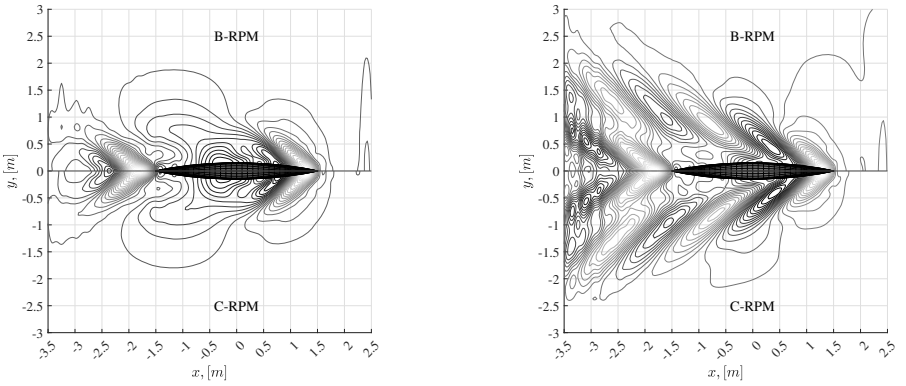

(a) (b)

Figure 4. Comparison of the wave pattern obtained with C-RPM and B-RPM for double-body flow solution at time instant $Ut/L = 0.5$ (a), and $Ut/L = 5.0$ (b), for $Fr = 0.45$.

applied to the free surface every 10 time steps; see [20] for further details. The filter's effect is observable as small spike-error peaks appearing in the forces' time histories, but it does not involve any change.

Figure 3 shows the heave force and pitch moment results obtained using both the C-RPM and B-RPM for the double-body flow solution. From the comparisons in Figures 3a and 4a, it is evident that the B-RPM, with a coarser geometric discretisation ($N_H = 550$ and $N_F = 1380$), provides results comparable to those of the C-RPM with a finer discretisation ($N_H = 770$ and $N_F = 1950$). The differences between the forces are partly due to the accuracy of the force computation, which is significantly higher through the B-RPM. Finally, Figure 4 compares the wave field generated by the model advancing at constant speed at two different time instants, computed using both the C-RPM and the B-RPM. Although calibration for the numerical beach is not always straightforward, as shown by the small reflection phenomena in Figure 4b, there is a strong agreement between the two wave patterns.

5. Conclusions

In this study, several methods were compared to solve the double-body flow problem, which is considered crucial for ensuring stable forced and free-motion simulations that require the integration of the equations of motion. Among the methods analyzed, the B-RPM demonstrated higher accuracy even with fewer panels for geometric discretization than the C-RPM. It also allows for the analytical computation of tangential derivatives via Eq. (10). This feature proved to be essential in free-motion simulations, where the accurate evaluation of the forcing term in the local flow problem, involving derivatives of the potential Φ, is critical for correctly integrating the equations of motion.

Preliminary simulations show that the developed model can solve the wave flow problem, provided the numerical beach is properly calibrated. The integral method for computing Φ_{zz}, the integral explicit method (IEM) for ψ_t, and the numerical filter on the free surface proved to be effective numerical tools.

This work provides a solid foundation for the ongoing extension of the B-RPM to free-motion simulations. The next step will be the gradual integration of nonlinear effects, to develop a B-RPM suitable for a nonlinear model based on the weak-scatterer assumption.

References

[1] Hess JL, Smith A. Calculation of potential flow about arbitrary bodies. Prog Aerosp Sci. 1967;8:1–138. doi:10.1016/0376-0421(67)90003-6.

[2] Taylor RE, Jefferys E. Variability of hydrodynamic load predictions for a tension leg platform. Ocean Eng. 1986;13(5):449–490. doi:10.1016/0029-8018(86)90033-8.

[3] King B, Beck R, Magee A. Seakeeping calculations with forward speed using time-domain analysis. In: Proceedings of the 17th Symposium on Naval Hydrodynamics; 1988 Aug 28–Sep 2; The Hague, Netherlands. Washington (DC): National Academy Press; 1989. p. 577–96. doi:10.17226/19077.

[4] Bingham HB. Simulating ship motions in the time domain [PhD thesis]. Cambridge (MA): Massachusetts Institute of Technology; 1994. Available from: http://hdl.handle.net/1721.1/12320.

[5] Sclavounos P, Nakos D. Stability analysis of panel methods for free-surface flows with forward speed. In: Battjes JA, editor. Proceedings of the 17th Symposium on Naval Hydrodynamics; 1988 Aug 28–Sep 2; The Hague, Netherlands. Washington (DC): National Academy Press; 1989. p. 173–194. doi:10.17226/19077.

[6] Pawlowski J. A nonlinear theory of ship motion in waves. In: Proceedings of the 19th Symposium on Naval Hydrodynamics; 1992 Aug 23-28; Seoul, Korea. Washington (DC): National Academy Press; 1994. p. 33–58.

[7] Gadd GE. A method for computing the flow and surface wave pattern around full forms. Trans R Inst Nav Archit. 1976;118:207–218.

[8] Dawson CW. A practical computer method for solving ship-wave problems. In: Proceedings of the 2nd International Conference on Numerical Ship Hydrodynamics; 1977 Sep 19–21; Berkeley, California. Berkeley (CA): University of California; 1977. p. 30–38.

[9] Nakos D, Kring D, Sclavounos P. Rankine panel methods for transient free surface flows. In: Patel VC, Stern F, editors. Proceedings of the 6th International Conference on Numerical Ship Hydrodynamics; 1993 Aug 2–5; Iowa City, Iowa. Washington (DC): National Academy Press; 1994. p. 613–634.

[10] Kring D. Time Domain Ship Motions by a Three-Dimensional Rankine Panel Method [PhD thesis]. Cambridge (MA): Massachusetts Institute of Technology; 1994. Available from: http://hdl.handle.net/1721.1/11939.

[11] Huang Y. Nonlinear Ship Motions by a Rankine Panel Method [PhD thesis]. Cambridge (MA): Massachusetts Institute of Technology; 1994. Available from: http://hdl.handle.net/1721.1/10336.

[12] Ogilvie TF, Tuck EO. A rational strip theory for ship motions. Part 1 [technical report]. Ann Arbor (MI): University of Michigan, Dept. of Naval Architecture and Marine Engineering; 1969. Report No.: 013.

[13] Katz J, Plotkin A. Low-speed aerodynamics. 2nd ed. Cambridge: Cambridge University Press; 2012. 613 p. doi:10.1017/CBO9780511810329.

[14] Nakos DE. Ship wave patterns and motions by a three-dimensional Rankine panel method [PhD thesis]. Cambridge (MA): Massachusetts Institute of Technology; 1990. Available from: http://hdl.handle.net/1721.1/13651.

[15] Newman JN. Distribution of sources and normal dipoles over a quadrilateral panel. J Eng Math. 1986;20:113–126.

[16] Israeli M, Orszag SA. Approximation of radiation boundary conditions. J Comput Phys. 1981;41(1):115–135.

[17] Kim Y. Computation of higher-order hydrodynamic forces on ships and offshore structures in waves [PhD thesis]. Cambridge (MA): Massachusetts Institute of Technology; 1999. Available from: http://hdl.handle.net/1721.1/79979.

[18] Holloway DS. Numerical stabilisation of motion integration. ANZIAM J. 2007;48(1):249–263.

[19] Nakos D, Sclavounos P. On steady and unsteady ship wave patterns. J Fluid Mech. 1990;215:263–288.

[20] Longuet-Higgins MS, Cokelet ED. The deformation of steep surface waves on water. I. A numerical method of computation. Proc R Soc Lond A. 1976;350:1. doi:10.1098/rspa.1976.0092.